Anais XIV Simpósio Brasileiro de Sensoriamento Remoto, Natal, Brasil, 25-30 abril 2009, INPE, p. 6517-6523.

A Census of the Cold Core eddies on the Brazil-Malvinas Confluence Region from TOPEX/POSEIDON altimeter: 1993-1998

Carlos Alessandre Domingos Lentini[1]
Wilton Zumpichiatti Arruda[2]

[1] Universidade Federal da Bahia – UFBA, Instituto de Física
Travessa Barão de Jeremoabo, s/n, Campus Ondina, Salvador - BA, Brasil
cadlentini@gmail.com
[2] Universidade Federal do Rio de Janeiro – UFRJ, Instituto de Matemática
Cid. Universitária, Bl. C, CT, C. P. 68530 – 21945-970 – Rio de Janeiro - RJ, Brasil
wilton@im.ufrj.br

Abstract. TOPEX/POSEIDON-derived sea height anomalies (SHA) are used in combination with a reduced gravity model to monitor the upper-layer thickness (ULT) in the Southwestern Atlantic. A survey of the cold-core eddies (CCEs) formed in the Brazil-Malvinas Confluence (BMC) between January 1993 and October 1998 is carried out using the ULT estimates. Forty-three CCEs are identified during a 6-year period, with an average of more than seven rings per year. The observed life span for the entire ensemble ranges between 30 and 160 days, with a mean of 90 days. After formation, these eddies generally move westward at a mean translation speed of 17 km/day. They have an average radius of 60 km and associated SHA of approximately 0.4 m. Our results suggest that the formation rate of CCEs is larger than previously thought, which is comparable to the formation of anticyclonic (warm core) eddies in the BMC. The average available potential energy is 9×10^{15} J. Computations of eddy volume anomaly show a mean value of 4.5×10^{12} m^3. Based on these calculations, a volume of approximately 0.6 Sv per ring of subantarctic waters are transfered to the subtropical gyre.

Keywords: altimetry, cold core eddies, Brazil-Malvinas Confluence ..

Palavras chave: altimetria, vórtices de núcleo frio, Confluência Brasil-Malvinas.

1. Introduction

At the Brazil-Malvinas Confluence (BMC), the Brazil Current (BC) and the Malvinas Current (MC) collide, forming a strong thermohaline front composed by a series of large-scale meanders and mesoscale eddies (Olson et al., 1988; Garzoli and Garraffo, 1989). After their separation from the coast, the BC continues flowing southward before looping back toward subtropical latitudes forming a large, quasi-stationary poleward lobe near the continental slope followed by secondary meanders that decay downstream. Anticyclonic and cyclonic eddies associated mainly with the first two meander undulations are then formed and released into subantarctic and subtropical regions, respectively. The BMC region is an area particularly suited for remote sensing techniques for two main reasons: Firstly, satellite-based sensors can provide a continuous, and synoptic monitoring required to adequately describe the complex mesoscale variability of the region. Secondly, unlike infrared imagery, altimeter data is unaffected by cloud coverage and can provide information on the vertical structure of the ocean dynamics if complemented by climatological hydrographic data and a diagnostic model (Goni et al., 1996, 1997; Goni and Johns, 2000; Lentini et al., 2006) Statistics of the eddy parameters is the first step to quantify possible contributions of these features to the distribution of heat and salt over the Southwestern Atlantic (SWA). While for the warm-core anticyclonic BC rings much attention has been given (Lentini et al., 2002, 2006a, 2006b) the cold-core cyclonic eddies (CCE) are still underestimated since there is neither a census of how many are formed a year nor a continuous history of their trajectories. Therefore, the goal of the present study is to carry out a synoptic study of the number of CCEs formed in the region (60°-20°W, 30°-50°S) which encompasses the BMC region. Here, these features are identified from their Upper Layer Thickness (ULT) signature as derived from the TOPEX/POSEIDON (T/P) altimeter Sea surface Height Anomalies (SHA) in combination with a reduced gravity model (Goni et al., 1997; Lentini et al., 2000, 2006b).

2. Data and Methods

The altimeter-derived SHA data and the climatological hydrographic data are the two main datasets used in this study. The T/P altimeter measures the SHA along groundtracks, which are separated 3 degrees longitudinally, and are repeated approximately every 9.91 days. The data used here is processed with the standard altimetric corrections (Cheney et al., 1994). The SHA values are referred to a 5-year mean (1993-1997) and interpolated into a 9 km alongtrack grid.

The altimeter-derived SHA and climatological data are used in conjunction with a local two-layer reduced gravity model to monitor the ULT, which in this study is defined to extend from the surface to the depth of the 8°C isotherm. The choice of the 8°C isotherm relies on previous hydrographic studies, where the relationship between this isotherm and the 0/1500 dynamic height anomaly is linear, with a correlation coefficient of 0.98% (Gordon, 1989; Garzoli and Garraffo, 1989). The SHA maps are interpolated onto a regular 0.25° grid using a Gaussian interpolation with an e-folding radius of interpolation with the same resolution. The SHA maps are converted into upper-layer thickness (ULT) maps using a reduced gravity model:

$$h(x, y, t) = \bar{h}(x, y) + \frac{g}{g'(x, y)}\eta(x, y, t), \tag{1}$$

where h is the ULT, η is the T/P SHA, g is the gravity, and g', and $\bar{h}$ are the reduced gravity and mean ULT both derived from the *World Ocean Atlas 1994* (Levitus and Boyer, 1994). This approach has been used with success to track and characterize other eddies: Agulhas eddies (Goni et al., 1997); North Brazil Current eddies (Goni and Johns, 2000), Brazil Current warm core eddies (Lentini et al., 2006). A total of 210 altimeter-derived ULT maps are constructed and used to visually identify the CCEs as well as their trajectories in the BMC region. The CCEs are identified as closed contours in the ULT (h) maps with length scales larger than 0.1° and decreasing ULT toward their centers. Their locations, estimated with an error not larger than 0.25^o, are placed at the point of minimum ULT. A figure with a snapshot of the ULT data can be seen in Lentini et al. (2006).

3. Results

A total of 43 CCEs are identified by using the above criteria between January 1993 and October 1998. Their distribution, lifetime, and translation speed are shown in Figure 1. The average number of CCEs formed per year is 7.2 ($\sim$ 7 eddies/year), with a marked increase in eddy formation starting in 1994 with an apex during 1996, which suggests a strong interannual variability (Fig. 1a). Most of the eddies can be identified for 2-3 months in the region of study (Fig. 1b). Based on a 17-month period of inverted echo sounder (IES) data in the BMC, Garzoli and Garraffo (1989) reported CCE lifetimes ranging from 20 to 60 days, in agreement with our results. The CCEs mean translation speed is 17 $\pm$ 10 km/day, ranging from 3 to 44 km/day (Fig. 1c). Considering the uncertainties in the location of the eddy center the error of these velocity estimates are of approximately 5 km/day. These values are in agreement with previously reported CCE speeds of 17-26 km/day in the BMC area (Garzoli and Garraffo, 1989; Gordon, 1989).

Figure 2 shows the ring trajectories during the 6-year study period. The squares (triangles) indicate the locations where the eddies are first (last) identified from the ULT maps. Most of these features (34 CCEs) are confined between 55-40°W and 42.5-33°S. After formation, the general tendency of their trajectories is westward across the region toward the continental slope,

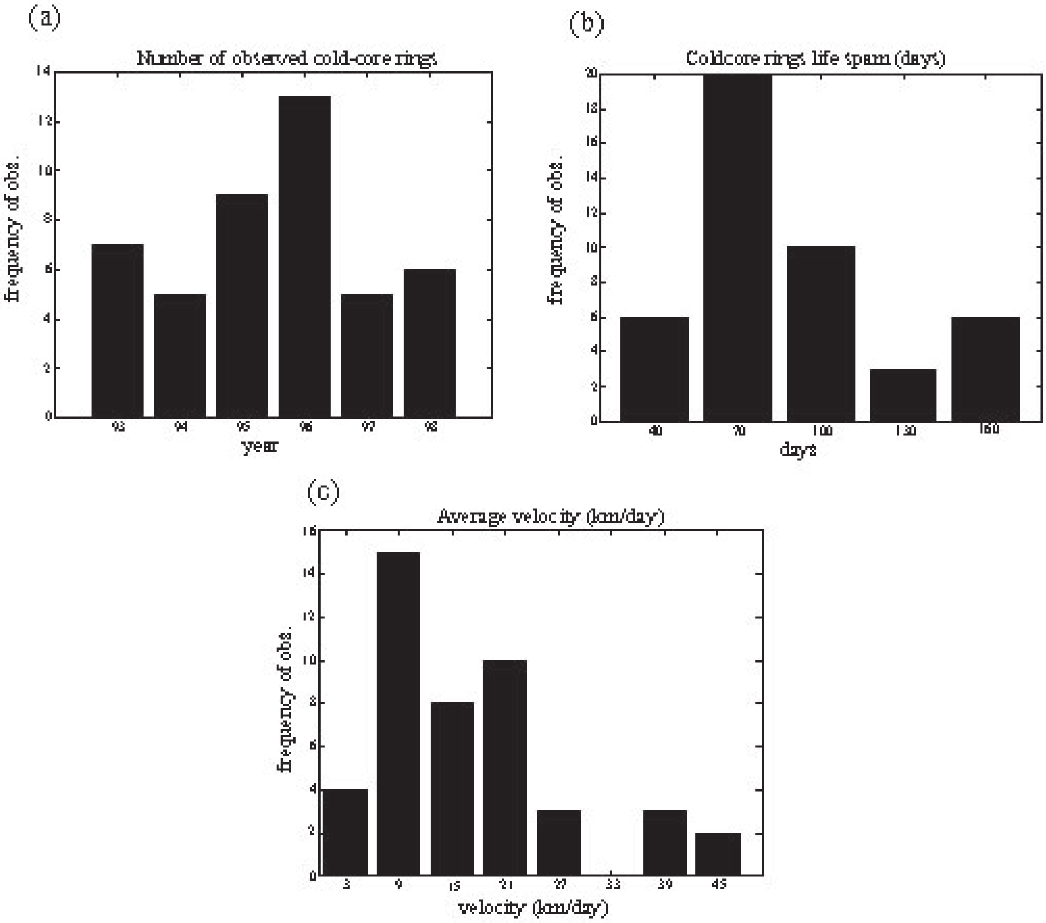

Figure 1: Histograms: (a) Monthly distribution of CCE formation from 1993 to 1998; (b) CCEs life time in days; (c) CCEs average translation speed in km day^{-1}.

except for years 1995 and 1996, where 2 and 5 CCEs translate toward to the north, respectively. None of the CCEs cross the continental slope ($\sim$ 1000 m isobath). In order to evaluate the eddy parameters we take a T/P groundtrack that most closely crosses its center on the ULT map. Then a Gaussian profile is fitted to the T/P alongtrack ULT (Goni et al., 1997)

$$h_1(r) = h_\infty - h_0 e^{-r^2/2L^2}, \tag{2}$$

where h_1 is the alongtrack Gaussian profile, h_∞ is the ULT reference value, h_0 is the ULT anomaly at the CCE center, and L is the eddy length scale. The least-square nonlinear fit to the Gaussian function (2) is then performed by letting L span a range of values between 10 and 200 km at intervals of 10 km. The rms error estimates for the non-linear fit for the entire ensemble ranges from 2 to 63 meters. The mean value of L is 65 $\pm$ 30 km, with most of the CCEs having horizontal length scales between 40 and 50 km. All the CCE parameters are summarized in Table 1. It is believed that the values of L, and h_1 computed here are slightly underestimated, since a T/P groundtrack seldom crosses an eddy at its center. If the CCRs are assumed to have a circular shape, the upper-layer volume anomaly (VOL) can be calculated as (Bennett, 1988; Goni et al., 1997):

$$VOL = 2\pi \int_0^\infty (h_1 - h_\infty) r \, dr = -2\pi h_0 L^2. \tag{3}$$

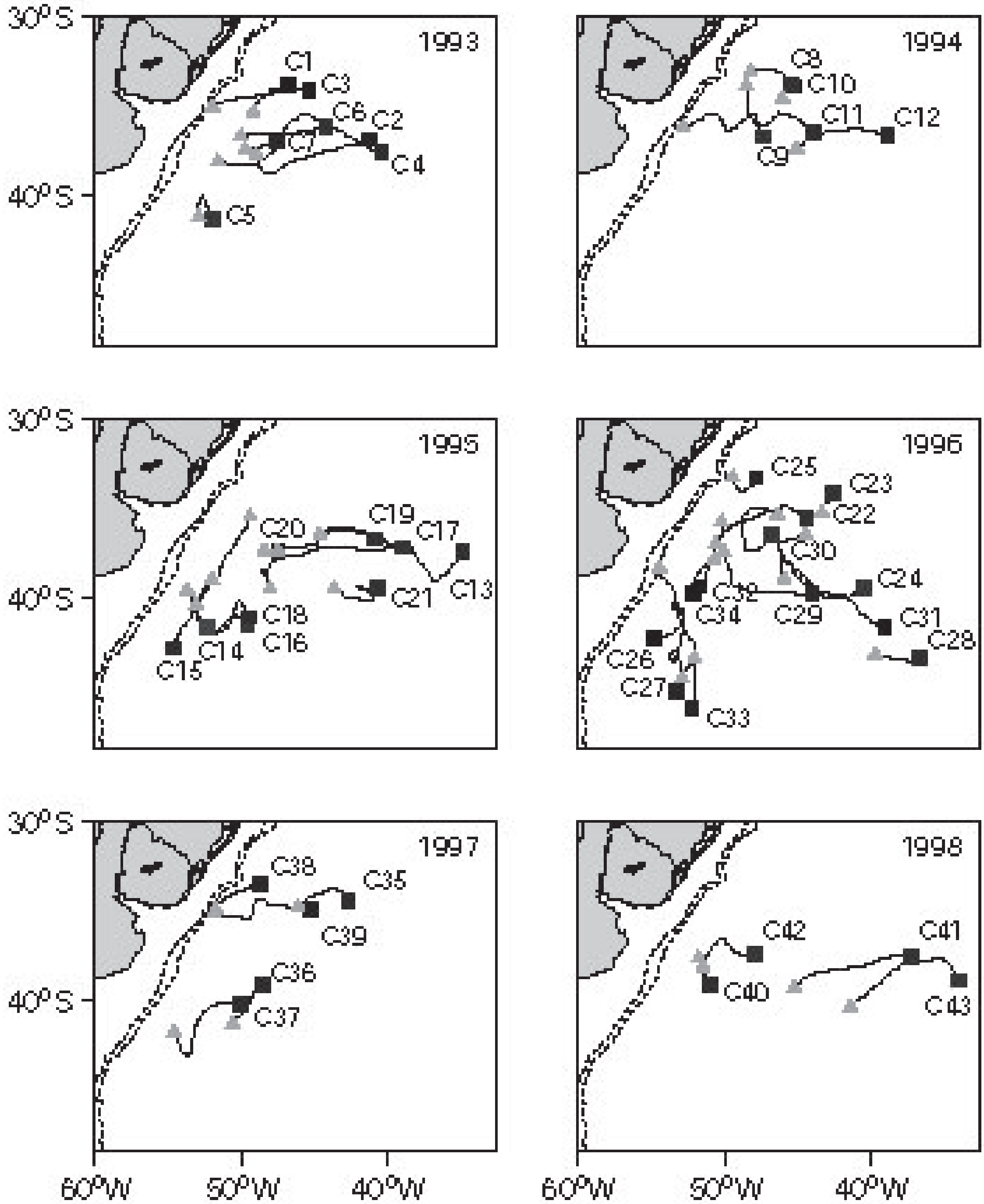

Figure 2: Trajectories of all 43 cyclonic eddies. The squares (triangles) indicate the location when the eddies are first (last) identified from the ULT maps. Differences in trajectories from year to year are suggestive of a marked interannual variability. None of the CCEs either remain in the region for more than a year or cross over the 1000 m isobath. Dashed lines are representative of the 200 m and 1000 m isobath.

Table 1: Parameters of the 44 observed CCEs. The table columns are the following: First: Each CCE is labeled as C*nn*-*yy*, where *yy* indicates the year where the eddy was first observed and *nn* the order of the observation within a year. Second: Month where each CCE was first detected in the ULT maps; Third: Maximum alongtrack Sea Height Anomaly (SHA); Forth: Upper layer thickness at the CCE center (h_0); Fifth: Upper layer thickness far away from CCE center (h_∞) Sixth: CCE length scale (L); Seventh: CCE volume anomaly (VOL); Eighth: CCE translations speed (Vel); Ninth: CCE Available Potential Energy (APE); Tenth: CCE life cycle (T).

Eddy	Month	SHA (cm)	h_0 (m)	h_∞ (m)	L (km)	VOL ($\times10^{12}$m^3)	Vel (km day^{-1})	APE ($\times10^{15}$J)	T (days)
C01-93	Jan 93	0.3	130	650	70	-4.1	24	2	80
C02-93	Apr 93	0.4	17	431	20	-0.05	10	0.002	100
C03-93	May 93	0.3	170	630	50	-2.7	22	2	80
C04-93	Jul 93	0.4	80	390	40	-0.8	11	0.2	110
C05-93	Sep 93	0.6	90	230	20	-0.2	19	0.07	80
C06-93	Oct 93	0.5	220	570	160	-35.4	20	26	70
C07-93	Dec 93	0.4	175	495	50	-2.8	13	2	110
C08-94	Jan 94	0.3	100	600	40	-1	17	0.3	110
C09-94	Jun 94	0.5	260	550	70	-8.1	12	7	150
C10-94	Jul 94	0.4	130	570	50	-2	38	0.8	40
C11-94	Aug 94	0.5	170	500	80	-6.8	14	4	110
C12-94	Nov 94	0.5	110	410	100	-6.9	7	2.5	90
C13-95	Jan 95	0.3	90	330	150	-13	4	4	160
C14-95	Jan 95	0.5	120	155	40	-1.2	23	0.5	70
C15-95	Apr 95	0.6	150	200	100	-9.4	13	4.7	130
C16-95	Jun 95	0.4	150	190	90	-7.5	10	3.7	150
C17-95	Apr 95	0.4	25	445	20	-0.06	8	0.005	120
C18-95	Jun 95	0.4	140	180	100	-8.6	9	4	150
C19-95	Aug 95	0.4	160	500	100	-10.1	9	5.4	90
C20-95	Dec 95	0.6	340	600	60	-7.6	19	8.6	70
C21-95	Dec 95	0.4	70	230	80	-3	5	0.7	60
C22-96	Jan 96	0.3	90	620	40	-0.9	20	0.3	80
C23-96	Mar 96	0.3	65	540	50	-1	36	0.2	30
C24-96	Apr 96	0.3	180	540	50	-2.9	12	1.8	80
C25-96	Apr 96	0.3	45	180	30	-0.3	22	0.04	90
C26-96	May 96	0.5	80	600	50	-1.3	19	0.4	90
C27-96	Jun 96	0.4	90	110	50	-1.4	38	0.4	30
C28-96	Jul 96	0.3	95	120	100	-6	10	1.9	70
C29-96	Jul 96	0.5	80	140	40	-0.8	16	0.2	60
C30-96	Oct 96	0.6	35	175	100	-2.2	23	0.3	70
C31-96	Oct 96	0.2	170	470	70	-5.3	6	3	90
C32-96	Nov 96	0.6	120	160	40	-1.3	25	0.5	70
C33-96	Nov 96	0.4	270	350	80	-10.7	16	9.6	80
C34-96	Dec 96	0.4	110	150	30	-0.6	42	0.2	40
C35-97	Apr 97	0.5	190	260	30	-1.1	11	0.7	120
C36-97	Feb 97	0.4	150	520	40	-1.5	16	0.7	80
C37-97	Sep 97	0.6	85	215	50	-1.3	10	0.4	150
C38-97	Oct 97	0.3	310	330	50	-4.9	44	5.1	50
C39-97	Dec 97	0.3	100	630	110	-7.3	12	2.4	150
C40-98	Feb 98	0.5	65	600	50	-1	28	0.2	60
C41-98	Feb 98	0.6	220	430	50	-3.4	9	2.5	60
C42-98	Feb 98	0.4	120	410	70	-3.7	21	1.5	80
C43-98	Mar 98	0.4	195	515	60	-4.4	3	2.9	80
Average		0.4	130	390	65	-4.5	17	2.6	90

The resulting values for VOL range from -0.05 to -36 $\times 10^{12}$ m^3, with an average of -4.5 $\times 10^{12}$ m^3. Also the Available Potential Energy (APE) is given by (Bennett, 1988; Olson, 1991; Goni et al., 1997)

$$APE = \pi \rho g' \int_0^\infty (h_1 - h_\infty)^2 r \, dr = \frac{\pi \rho g' h_0^2 L^2}{2}. \tag{4}$$

The estimated values of APE are shown in Table 1. These values are calculated for a g' = 0.013 m/s^2 and ρ = 1.0265 g/cm^3. The APE values for the entire ensemble range from values as low as 0.01 (C38-97) to 72 $\times 10^{15}$ J (C39-97), with a mean value of 9 $\times 10^{15}$ J. Garzoli and Garraffo (1989) and Gordon (1989) reported APE values of 6.5 and 23 $\times 10^{15}$ J, respectively, which corroborate our results.

4. Conclusions

Under the assumption of subantarctic waters trapped in the core of the cyclonic eddies, a volume equivalent to approximately 0.6 Sv per ring, may account for at least 3 Sv per year ($\sim$ 5 eddies per year) of intergyre exchange in the Confluence. Despite some uncertainties on eddy identification and characterization, these results seem to reflect the eddies' properties when compared to more limited in-situ observations (Olson, 1991; Table 1). However, the role played by these features in the adjacent environment is still poorly understood. Since altimetric observations cannot directly determine the vertical structure of these mesoscale features, further *in situ* observations are undoubtedly needed to quantify the exchange of physical properties between adjacent environments. Therefore, a combination of ship-based measurements and remote sensing techniques are necessary to fully address these issues.

Acknowledgments

The authors also would like to thank the Brazilian Research and Technology Council (CNPq) for funding the BACANA and VARICONF Projects, grants 478398/2006-9 and 476472/2006-7, respectively.

5. References

Cheney, R.; Miller, L; Argreen, R.; Doyle, N.; Lillibridge, J. TOPEX/POSEIDON: The 2-cm Solution. **Geophysical Reasearch Letters** , v. 99, p. 24555-24564, 1994.

Garzoli, S. L. ; Garraffo, Z. S. Transports, frontal motions and eddies at the Brazil-Malvinas Currents Confluence. **Deep-Sea Research**, v. 36, p. 681-703, 1989.

Goni, G. J.; Johns, W. E. A Census of North Brazil Current rings observed from TOPEX/POSEIDON altimetry: 1992-1998. **Geoghysical Research Letters**, v. 28, n. 1, p. 5555-6666, 2000.

Goni, G. J., Garzoli, S. L. ; Roubicek, A.; Olson, D. B. ; Brown, O. B. Agulhas ring dynamics from TOPEX/POSEIDON satellite altimeter data. **Journal of Marine Research**, v. 55, p. 861-883, 1997.

Gordon, A. L. Brazil-Malvinas Confluence - 1984, **Deep-Sea Research**, v. 36, p. 359-384, 1989.

Lentini, C. A. D., Olson, D. B.; Podest/'a, G. P. Statistics of Brazil Current rings observed from AVHRR: 1993 to 1998. **Geophysical Research Letters**, v. 29, n. 16, art. n. 1811, 2002.

Lentini, C. A. D.; Goni, G. J.; Olson, D. B.; Investigation of Brazil Current rings in the Confluence region, **Journal of Geophysical Research-Oceans**, v. 111, C6, C06013, 2006

Levitus, S.; Boyer, T. P. **World ocean atlas, Volume 4: Temperature**. Washington, D.C., USA: NOAA Atlas NESDIS 4, U.S. Govt. Print. Off., 1994. 117 p.

Olson, D. B., Rings in the ocean. **Annual Reveviews of Earth Planetary Sciences**, v. 19, p. 283-311, 1991.

Olson, D. B.; Podestá, G. P.; Evans, R. H.; Brown, O. B. Temporal variations in the separation of Brazil and Malvinas Currents. **Deep-Sea Research**, v. 35, p. 1971-1990, 1988.